Published in final edited form as:
Anal Chem. 2007 April 1; 79(7): 2735–2744. doi:10.1021/ac062089i.

Probing Heterogeneous Electron Transfer at an Unbiased Conductor by Scanning Electrochemical Microscopy in the Feedback Mode

Hui Xiong, **Jidong Guo**, and **Shigeru Amemiya***
Department of Chemistry, University of Pittsburgh 219 Parkman Avenue, Pittsburgh, Pennsylvania, 15260

Abstract

The theory of the feedback mode of scanning electrochemical microscopy is extended for probing heterogeneous electron transfer at an unbiased conductor. A steady-state SECM diffusion problem with a pair of disk ultramicroelectrodes as a tip and a substrate is solved numerically. The potential of the unbiased substrate is such that the net current flow across the substrate/solution interface is zero. For a reversible substrate reaction, the potential and the corresponding tip current depend on SECM geometries with respective to the tip radius including not only the tip–substrate distance and the substrate radius but also the thickness of the insulating sheath surrounding the tip. A larger feedback current is obtained using a probe with a thinner insulating sheath, enabling identification of a smaller unbiased substrate with a radius that is approximately as small as the tip radius. An intrinsically slow reaction at an unbiased substrate as driven by a SECM probe can be quasi-reversible. The standard rate constant of the substrate reaction can be determined from the feedback tip current when the SECM geometries are known. The numerical simulations are extended to an SECM line scan above an unbiased substrate to demonstrate a “dip” in the steady-state tip current above the substrate center. The theoretical predictions are confirmed experimentally for reversible and quasi-reversible reactions at an unbiased disk substrate using disk probes with different tip radii and outer radii.

Scanning electrochemical microscopy (SECM) is a powerful electroanalytical technique for probing interfacial reactions at a variety of substrates.[1–3] SECM is versatile partially because the substrates do not require an electrical connection to an external circuit,[4] which is in contrast to traditional electroanalytical techniques.[5] SECM measurement of unbiased substrates is advantageous when the substrates can not be conveniently connected to an external circuit or when the application of a potential causes an undesirable effect on the substrates. In particular, SECM feedback mode has been used in recent studies of charge transport at unbiased nanostructured systems such as metal nanoparticle arrays/films,[6–13] carbon nanotube network,[14] individual nanobands,[15] an array of protein nanopores,[16] and nanometer-thick polymer films.[17–20]

A heterogeneous electron transfer process at an unbiased conductor can be studied by SECM in the feedback mode, where the process is driven and monitored using an ultramicroelectrode (UME) probe. Consider a disk UME positioned within a short distance (usually within about the tip diameter) of a disk-shaped conductive substrate (Figure 1). The UME tip is biased for electrolysis of a redox-active mediator, O, in the electrolyte solution ($O + ne^- \rightarrow R$; process 1 in Figure 1). The tip-generated species, R, diffuses to and reacts at the surface of the conductive

*To whom correspondence should be addressed. E-mail: amemiya@pitt.edu. Fax: 412-624-5259.

substrate directly under the tip (process 2). The mediator regeneration process at the substrate can be monitored as enhancement of the tip current. Steady-state mediator regeneration at an unbiased substrate is coupled with electron transport in the substrate and mediator electrolysis at the exterior surface of the substrate (process 3), resulting in a mixed potential of the substrate.

A semi-quantitative model for unbiased disk substrates predicts that mediator diffusion limits an intrinsically fast mediator regeneration at a sufficiently large or small substrate.[21] When the area of an unbiased substrate is at least 1000 times larger than the tip area, a sufficiently large exterior surface of the substrate is exposed to the bulk solution so that the substrate potential is set by the bulk concentration of the mediator to drive the mediator regeneration to the diffusion limit. Therefore, as the tip is brought to the substrate surface, the tip current that is controlled by mediator diffusion between the tip and the substrate increases monotonically, yielding an approach curve (a plot of the tip current versus the tip-substrate distance) based on pure positive feedback. On the other hand, when the tip size is comparable to the substrate size, no mediator regeneration is expected at the steady state.[21] In this case, the tip current is limited by mediator diffusion from the bulk solution to the tip. In fact, a pair of disk Pt UMEs with the same diameter were used as a substrate and a probe to demonstrate an approach curve based on pure negative feedback, where the tip current decreases monotonically to zero at shorter tip-substrate distances.[22] During the tip approach, the open circuit potential of the unbiased substrate varies with the tip-substrate distance such that no mediator regeneration occurs on the substrate surface.[23]

SECM feedback can be controlled also by electron transfer at an unbiased substrate. Mediator electrolysis at the exterior surface of the substrate controls the feedback current when the substrate area is larger than the tip area by a factor of less than 1000.[21] At an unbiased disk substrate of intermediate size, a smaller feedback current is obtained using a disk probe with a larger diameter.[24] Moreover, the feedback current can be controlled by kinetics of mediator regeneration at the substrate.[21] A smaller feedback current is expected for an intrinsically slower reaction at an unbiased substrate. Recently, the theory for biased substrates[25] was used to determine electron-transfer rates at unbiased substrates from a kinetically limited tip current.[26–28] The assumption of irreversible kinetics in the analyses, however, is not valid for an unbiased substrate where both regeneration and electrolysis of a mediator occur. In addition, the open circuit potential of an unbiased substrate varies with the tip-substrate distance to give a distance-dependent reaction rate, which is in contrast to a constant reaction rate with a biased substrate at a fixed potential.

Here we report on numerical simulations of SECM feedback effects at unbiased substrates with high conductivity. A steady-state SECM diffusion problem is solved numerically for a disk probe positioned above an unbiased disk substrate, where the substrate potential is such that the net current flow across the substrate/solution interface is zero. Effects of the substrate size and heterogeneous electron transfer kinetics on the mixed potential of the substrate and the tip current are studied theoretically and experimentally. The SECM feedback is found to depend also on the thickness of the insulating layer surrounding the metal disk probe, which hinders mediator diffusion from the bulk solution to the substrate. The numerical simulations are extended to an SECM line scan above an unbiased disk substrate to demonstrate that the tip current is less enhanced above the substrate center than above the substrate edge, resulting in a current “dip.”

THEORY

Model

An SECM diffusion problem with a pair of disk-shaped UMEs as a probe and a substrate is defined in a cylindrical coordinate (Figure 2). The origin of the coordinate axes is set at the

center of the disk UME probe. The *r* and *z* coordinates are in directions that are parallel and normal to the disk probe surface, respectively. The disk substrate electrode is faced in parallel to the probe surface such that the substrate center is directly under the probe center. Disk radii of the probe and substrate electrodes are given by *a* and *b*, respectively. An insulating sheath with the outer radius of r_g surrounds the tip. The outer substrate radius corresponds to 100*a* and limits the simulation space in the r-direction. The simulation space behind the tip is defined by the value of 20*a*, which is large enough to accurately simulate back diffusion of a mediator at a probe with RG < 10.[29]

Initially, the solution phase contains only one redox-active mediator, O, which is reduced to R at the tip (O + *n*e → R). Steady-state diffusion of O in the solution phase can be expressed as

$$\frac{\partial c(r,z)}{\partial t}=D\left[\frac{\partial^2 c(r,z)}{\partial r^2}+\frac{1}{r}\frac{\partial c(r,z)}{\partial r}+\frac{\partial^2 c(r,z)}{\partial z^2}\right]=0 \quad (1)$$

where $c(r,z)$ is the steady-state local concentration of the mediator. The initial condition is given by

$$c(r,z)=c_0 \quad t=0 \quad \text{(in the electrolyte solution)} \quad (2)$$

The diffusion coefficients of O and R are assumed to be the mean value so that mathematical treatment is restricted to the concentration of O.

The disk SECM probe is biased such that mediator electrolysis at the tip is diffusion-limited in the bulk solution. When the tip is positioned far from the substrate, a steady-state limiting current, $i_{T,\infty}$, is obtained as

$$i_{T,\infty}=4xnFDc_0a \quad (3)$$

where *x* is a function of RG (= r_g/a),[30] *F* is the Faraday constant, and *D* and c_0 are the diffusion coefficient and concentration of the redox mediator in the bulk solution.

The substrate is assumed to be conductive enough to maintain a uniform potential within the phase. A steady-state current across the unbiased substrate/solution interface, i_S, is zero as given by

$$i_s=2\pi nFD\int_0^b r\left[\frac{\partial c(r,d)}{\partial z}\right]dr=0 \quad (4)$$

The substrate surface boundary condition depends on electrochemical reversibility of the substrate reaction. For a reversible reaction, the boundary condition is given by

$$E=E^{0\prime}-\frac{RT}{nF}\ln\frac{c_0-c(r,d)}{c(r,d)} \quad (5)$$

where *E* is the open circuit potential of the unbiased substrate, and $E^{0'}$ is the formal potential. When the substrate reaction is kinetically limited, only one-step, one-electron transfer processes (*n* = 1) are considered

$$\mathbf{O}+\mathrm{e}\underset{k_{b,s}}{\overset{k_{f,s}}{\rightleftharpoons}}\mathbf{R} \quad (6)$$

where $k_{f,s}$ and $k_{b,s}$ are the first-order heterogeneous rate constants. The rate constants are given by the Butler-Volmer relations[31]

$$k_{f,s}=k^0\exp[-\alpha F(E-E^{0\prime})/RT] \tag{7}$$

$$k_{b,s}=k^0\exp[(1-\alpha)F(E-E^{0\prime})/RT] \tag{8}$$

where k^0 is the standard rate constant, and α is the transfer coefficient. The corresponding substrate surface boundary condition is given by

$$D\left[\frac{\partial c(r,z)}{\partial z}\right]_{z=d}=-k_{f,s}c(r,d)+k_{b,s}[c_0-c(r,d)] \quad (0<r<b, z=d) \tag{9}$$

A dimensionless rate constant, K, for the substrate reaction is defined by

$$K=\frac{k^0 a}{D} \tag{10}$$

The other boundary conditions are given by

$$c(r,0)=0 \quad 0<r<a \quad \text{(tip surface)} \tag{11}$$

$$\left[\frac{\partial c(r,z)}{\partial z}\right]_{z=0}=0 \quad a<r<r_g \quad \text{(insulator)} \tag{12}$$

$$\left[\frac{\partial c(r,z)}{\partial r}\right]_{r=r_g}=0 \quad -20a<z<0 \quad \text{(insulator)} \tag{13}$$

$$c(r,z)=c_0 \quad r_g<r<100a, z=-20a \text{ and } r=100a, -20a<z<d \quad \text{(simulation space limits)} \tag{14}$$

$$\left[\frac{\partial c(r,z)}{\partial r}\right]_{r=0}=0 \quad 0<z<d \quad \text{(axis of symmetry)} \tag{15}$$

The SECM diffusion problem was solved in a dimensionless form by COMSOL Multiphysics® version 3.2 (COMSOL, Inc., Burlington, MA), which applies the finite element method (see Supporting Information). An open circuit potential of the substrate was chosen such that the substrate current is less than 1% of $i_{T,\infty}$, to satisfy eq 4. The corresponding tip current, i_T, is given by

$$i_T=2\pi nFD\int_0^a r\left[\frac{\partial c(r,0)}{\partial z}\right]dr \tag{16}$$

Plots of the tip current and substrate potential versus the tip-substrate distance give current and potential approach curves, respectively. Calculation at each distance took 1–10 s on a workstation equipped with a Xeon 3.0 GHz processor unit and 5.0 GB RAM with Linux.

Finite Substrate Effect for Reversible Reaction

For a reversible reaction at an unbiased finite substrate, the feedback is controlled by mediator electrolysis at the limited exterior surface of the substrate (process 3 in Figure 1). Both current and potential approach curves depend on two dimensionless parameters, b/a and RG. The relative size of the substrate, b/a, determines the area of the exterior substrate surface that is exposed to the bulk solution for the mediator electrolysis. The relative thickness of the insulating sheath, RG, determines diffusional accessibility of the exterior surface to the mediator in the bulk solution.

Current and potential approach curves at unbiased disk substrates with different radii were calculated for a SECM probe with a standard RG of 10. At a small substrate with $b/a < 2$, the current approach curve coincides with a negative approach curve as obtained at an insulating substrate (Figure 3a). In this case, an open circuit potential of the substrate is so negative that no mediator regeneration occurs (Figure 3b), resulting in pure negative feedback. In previous SECM studies, disk-shaped tip and substrate electrodes with the same radius was considered to demonstrate pure negative feedback at an unbiased substrate.[22,23] At a large substrate with $b/a \geq 30$, the current approach curve is very similar to a curve based on pure positive feedback. The potential of the large substrate is positive enough to drive the mediator regeneration to the diffusion limit. The range of b/a that results in pure positive feedback agrees with a semi-quantitative estimation.[21] For an intermediate substrate radius of $2 < b/a < 30$, the tip current is enhanced more with a larger substrate, where a larger exterior surface of the substrate with more positive potential is available for mediator electrolysis. Interestingly, the current approach curve changes dramatically when the substrate radius is comparable to the thickness of the insulating sheath around the tip ($b/a \sim \text{RG} = 10$). At a substrate with $b/a = \text{RG}$, the tip current increases monotonically as the tip-substrate distance decreases. When the substrate is slightly smaller than the outer diameter of the tip ($b/a = 9$), the tip current is suppressed significantly at short tip–substrate distances.

The dependence of the feedback current on the substrate size can be explained by considering localized distribution of interfacial mediator flux on the substrate surface (Figure 3c). At a short tip–substrate distance of $d/a = 0.5$, the flux based on mediator regeneration is localized on the substrate surface directly under the tip. This result indicates that the substrates with $b/a = 9$–15 are large enough to collect most tip-generated species. In fact, collection efficiency is close to unity at a biased substrate that is a few times larger than the tip, resulting in pure positive feedback.[32] In contrast to the biased substrate, however, pure positive feedback is not obtained at the unbiased substrates with the intermediate sizes, where mediator regeneration is coupled with mediator electrolysis at the exterior surface of the substrates. Importantly, the flux based on the mediator electrolysis is localized at the substrate edge. The edge of a larger substrate is more accessible to the mediator in the bulk solution, enhancing the mediator regeneration and subsequently the tip current. Moreover, mediator diffusion from the bulk solution to the substrate edge is significantly hindered by the insulating sheath of the tip, when the substrate radius is comparable to or smaller than the tip outer radius. Thus, a large RG effect on the tip current is observed for $\text{RG} \sim b/a$.

RG Effect on the Detectable Substrate Size

The RG effect at an unbiased substrate, which has not been considered in any previous SECM study,[21,23,33] was further confirmed by simulating approach curves for probes with different outer diameters (Figure 4a). With $b/a = 10$, current approach curves change from negative to positive as RG changes from 50 to 1.1. This RG effect on the tip current at an unbiased conductive substrate is much larger than the well-known RG effect at an insulating substrate,[34] where the tip current varies with RG, but only decreases monotonically as the tip is brought closer to an insulating substrate.

A smaller unbiased substrate on an insulating plane can be resolved using a probe with a thinner insulating sheath, which gives a larger feedback current. When a probe with a small RG of 1.1 is brought into the proximity of an unbiased substrate with $b/a \geq 1.1$, the tip current is significantly larger than that at an insulating substrate (Figure 4b). The substrate size of $b/a = 1.1$ is half of the smallest size of an unbiased substrate that can be detected using a probe with RG = 10 (Figure 3a). The b/a values of 1.1–2.0, however, are approximately 10 times larger than the corresponding values of 0.1–0.2 for the smallest biased substrate that is detectable in the feedback mode. This result is due to the need for an exterior surface of an unbiased substrate,

where mediator electrolysis occurs to balance mediator regeneration under the tip. It should also be noted that, even using the probe with a small RG of 1.1, pure positive feedback is obtained at a large unbiased substrate with $b/a > 30$, which is much larger than the corresponding biased substrate ($b/a > \sim 1$).[35] The range of $b/a > 30$ as required for a probe with RG of 1.1–10 is consistent with the semi-quantitative estimation,[21] which is a good approximation when the substrate radius is sufficiently larger than the tip outer radius.

Kinetically Limited Approach Curves

The tip current and substrate potential also depend on the kinetics of heterogeneous electron transfer at an unbiased substrate. Compared with biased substrates, theoretical treatment of kinetic effects at unbiased substrates is more complicated. First, quasi-reversible kinetics must be considered at an unbiased substrate, where both mediator electrolysis and regeneration occur at the steady state to maintain the charge balance in the substrate. Thus, an approximation of irreversible kinetics[25] is not valid for an unbiased finite substrate. Second, the corresponding rate constants must be given as a function of the substrate potential, which varies with the SECM geometries with respect to the tip radius including the tip–substrate distance, substrate radius, and tip outer diameter. Each rate constant is defined by two kinetic parameters, k^0 and a, and the overpotential, $E - E^0$, on the basis of the Butler-Volmer model (see eqs 7 and 8).

At a large substrate with $b = 30a$, a current approach curve for a substrate reaction with $K > 10$ is based on pure positive feedback ($\alpha = 0.5$ in Figure 5a). A current approach curve for smaller K is more negative because of a kinetic limitation. With $K < 2.5 \times 10^{-4}$, a current approach curve is similar to a negative one as observed at an insulating substrate, indicating that the substrate reaction is intrinsically too slow to regenerate the mediator. The substrate potential is significantly more positive than E^0 at the large substrate and becomes more positive for a slower reaction at short tip–substrate distances (Figure 5b). Due to the large overpotential at the large substrate, the transfer coefficient also affects the tip current and substrate potential substantially (see Supporting Information). Thus, the determination of K (or a) at a large substrate requires prior knowledge of a (or K). Alternatively, a pair of approach curves obtained in solutions containing species O or R will allow the determination of both parameters.

Current and potential approach curves at a smaller substrate ($b/a = 9$) are sensitive to K but not to α (see Supporting Information). A range of K for a kinetic limitation with the smaller substrate is very similar to that at the larger substrate. For both substrates, the largest K value that results in a quasi-reversible substrate reaction is equal to 10, corresponding to $k^0 = 0.1$–1.0 cm/s for standard values of $\alpha = 1$–10 μm and $D = 1.0 \times 10^{-5}$ cm^2/s (see eq 10). Either tip current or substrate potential at the small substrate is not sensitive to a, because of smaller overpotentials. Therefore, K can be estimated directly from an approach curve at a small substrate, where a can not be addressed.

RG Effect on Line Scan

A steady-state tip current in a line scan above an unbiased disk substrate was obtained numerically for reversible substrate reactions. The diffusion problem was solved in a three-dimensional coordinate as reported elsewhere.[15] Interestingly, tip current is more enhanced above the substrate edge than above the center, resulting in a line scan with a current dip. For instance, such a current dip is shown in a line scan above an unbiased substrate with $b/a = 5$ as obtained using a probe with RG = 10 (solid line in Figure 6a). A larger tip current is obtained above the substrate edge, where the mediator in the bulk solution is more accessible to the substrate through the opposite side of the edge (Figure 6b). When the probe is positioned directly above the substrate center, mediator diffusion from the bulk solution to the whole substrate edge is uniformly hindered by the insulating sheath, resulting in the current dip. In

fact, a current dip above the substrate center is much smaller for a probe with RG = 4 (dotted line in Figure 6a).

A similar current dip above the substrate center was reported previously in SECM images using a pair of 25 μm-diameter Pt disk electrodes both as a probe and an unbiased substrate.[22] Line scans in the images, however, were asymmetric with respect to the substrate center; the tip current above the edge before probe's passing the center was larger than that above the opposite side of the edge after passing the center. The asymmetric line scan with a current dip was ascribed to a transient current response. In our numerical simulations, symmetric line scans with a current dip were obtained at the steady state. Unfortunately, numerical simulations of a transient tip current at an unbiased substrate are difficult, because the mixed potential of the substrate also varies with time. Therefore, we will demonstrate experimentally that a current dip is still observed in the steady-state line scan at slow scan rates, where the non-steady-state asymmetric response is not observed.

EXPERIMENTAL SECTION

Chemicals

Tris(1,10-phenanthroline)cobalt (II), $Co(phen)_3^{2+}$, and 1,1′-ferrocenedimethanol (Strem Chemicals, Newburyport, MA) were used as redox mediators. $Co(phen)_3^{2+}$ was obtained from stoichiometric amounts of $CoCl_2 \cdot 6H_2O$ (Fisher Chemical, Fair Lawn, NJ) and 1,10-phenanthroline (Aldrich, Milwaukee, WI) in 0.1 M KCl. The mediator solutions were prepared under nitrogen in a glove bag (Aldrich) to avoid oxidation of the mediator by oxygen.[36] All reagents were used as received. All aqueous solutions were prepared with 18.3 MΩ·cm deionized water (Nanopure, Barnstead, Dubuque, IA).

Electrode Fabrication and Characterization

A ~33 μm-diameter carbon fiber disk substrate electrode, and 6, 10, and 25 μm-diameter Pt disk probes were fabricated as described previously.[37,38] The Pt wires were obtained from Goodfellow (Devon, PA). The carbon fiber was purchased from World Precision Instruments (Sarasota, FL). The diameter of the inlaid carbon fiber electrode was determined from a limiting current of a steady-state voltammogram using eq 3 with $x = 1$. The voltammogram was also used to determine E^0. The tip radius and insulating sheath thickness of the Pt probes were determined from current approach curves at an insulating Teflon substrate[29,39] measured using a home-built SECM setup[40] and were also checked by optical microscopy. For probes with RG ~ b/a, the RG values could be determined more accurately using the carbon fiber substrate at open circuit potential than using the insulating substrate (see Results and Discussion).

SECM Measurements

Approach curve and imaging experiments were performed using a commercial SECM instrument with close-loop piezoelectric motors, CHI 910B (CH Instruments, Austin, TX). The SECM instrument was placed on a vibration isolation platform (model 63-533, TMC, Peabody, MA). A two-electrode setup was employed with a 1 mm-diameter AgCl-coated Ag wire serving as a reference/counter electrode and a Pt disk electrode as a SECM probe. The open circuit potential of the carbon fiber substrate was measured with respect to another Ag/AgCl reference electrode using a 16-channel potentiometer (Lawson Labs Inc., Malvern, PA). The tip current and the open circuit potential of the substrate were measured simultaneously during tip approach to obtain current and potential approach curves, respectively. For approach curve measurements, a probe was positioned directly above the substrate as shown in Figure 2, where the largest tip current was obtained by setting the substrate potential for diffusion-limited

mediator regeneration.[23] SECM measurements with $Co(phen)_3^{2+}$ were carried out in the globe bag filled with nitrogen.

RESULTS AND DISCUSSION

Finite Substrate Effect

Effects of the substrate size on the tip current and substrate potential were examined using 1,1′-ferrocenedimethanol as a reversible mediator. A ~33 um-diameter carbon fiber electrode was used as a model conductive substrate without the external control of the potential. Current approach curves were obtained using 6, 10, and 25 μm-diameter disk Pt probes with RG = 7.5, 8.0, and 10, respectively (Figure 7a). Simultaneous measurements of an open circuit potential of the substrate (Figure 7b) did not affect the tip current. For a Pt probe with a smaller diameter, the tip current is enhanced more, indicating more efficient mediator regeneration at the substrate surface directly under the tip. With a smaller probe, a larger exterior surface of the substrate is available for oxidation of the ferrocene mediator so that the substrate potential is more negative. The more negative substrate potential results in more efficient reduction of the tip-generated ferrocenium at the substrate, giving the larger tip current.

The current and potential approach curves were analyzed to quantify the feedback effect at the unbiased conductive substrate. The current approach curves fit well with theoretical curves for a reversible substrate reaction (Figure 7a). The reversible behavior is consistent with a large standard rate constant of ferrocene derivatives at carbon electrodes, e.g., k^0 = 0.19 cm/s for ferrocenemethanol at a glassy carbon electrode.[41] The geometrical parameters of *b*/*a* and RG in the best fits are consistent with those determined by optical microscopy. The current approach curve obtained with the 25 μm-diameter probe also fits with a theoretical curve for an insulating substrate, indicating that the unbiased substrate is too small in comparison with the probe diameter to regenerate the mediator. The geometrical parameters can be used to obtain theoretical potential approach curves that fit well with the experimental curves (Figure 7b). This result indicates that the measurement of the substrate potential is not necessary for analysis of the current approach curve. Therefore, theoretical analysis is also possible with an unbiased substrate that can not be connected to an external circuit for potential measurement.

RG Effect

The quantitative theory of SECM feedback at an unbiased substrate predicts that both tip current and substrate potential depend on the tip outer radius, especially when the radius is comparable to the substrate radius (Figure 3a). The insulating sheath around the tip hinders mediator diffusion from the bulk solution to the substrate edge, where mediator electrolysis occurs to maintain the steady-state mediator regeneration under the tip (Figure 3c). The RG effect was studied experimentally using a 10 μm-diameter disk Pt probe with a thin insulating sheath. With 1,1′-ferrocenedimethanol as a reversible mediator, the tip current increased monotonically as the tip was brought to the unbiased carbon fiber substrate (red solid line in Figure 8a). This result is in contrast to the negative approach curve obtained using the 10 μm-diameter probe with RG = 8 (blue solid line in Figure 7a), confirming that a probe with smaller RG gives a larger feedback current at an unbiased substrate. The substrate potential is more negative for the probe with smaller RG (Figure 8b), resulting in a larger feedback current based on more facilitated reduction of the tip-generated ferrocenium.

The positive current approach curve obtained using the 10 μm-diameter probe with small RG fits well with a theoretical curve for a reversible substrate reaction (Figure 8a), yielding RG = 3.3. Theoretical curves with a slightly smaller or larger RG value of 3.1 or 3.5, respectively, do not fit with the experimental curve. The theoretical tip current is highly sensitive to RG in this case, because the substrate diameter of 34 μm is comparable to the tip outer diameter of

33 μm. On the other hand, the effect of the tip outer diameter on the corresponding potential approach curves is small (Figure 8b) because the substrate potential depends on the logarithm of the mediator concentration at the substrate surface for a reversible reaction (see eq 5).

The RG effect at an unbiased substrate is much more significant than the well-known RG effect at an insulating substrate.[29,34,42] A negative current approach curve at a Teflon substrate as obtained using the probe with RG = 3.3 (black solid line in Figure 8a) fits with any of the theoretical curves with RG = 3.1–3.5 at an insulating substrate, which nearly superimpose each other. It should also be noted that the current approach curve obtained using the 10 μm-diameter probe with RG = 3.3 is more positive than that obtained with the 6 μm-diameter probe with RG = 7.5 (Figure 7a) because the outer diameter of the former probe is smaller than that of the latter. The RG effect, however, is also significant in the current approach curve with the 6 μm-diameter probe, where the maximum current at $d/a = 0.8$ can not be reproduced theoretically with an RG of 7 or 8.

Quasi-Reversible Kinetics at an Unbiased Substrate

The kinetics of heterogeneous electron transfer at an unbiased substrate affects the tip current and substrate potential. A current approach curve with $Co(phen)_3^{2+}$ at the unbiased carbon fiber substrate (red solid line in Figure 9a) is more negative than that with 1,1′-ferrocenedimethanol (black solid line). The latter curve fits well with a theoretical curve for a reversible substrate reaction with $b/a = 3.2$ and RG = 2.0, where a 10 μm-diameter probe with a small RG was used to obtain a large feedback current. The current approach curve with $Co(phen)_3^{2+}$ fits well with a theoretical curve for a quasi-reversible substrate reaction with the same b/a and RG values, yielding $K = 0.52$ with $\alpha = 0.5$. The theoretical curve does not depend on a substantially because the open circuit potential of the substrate during the tip approach is close to the formal potential (Figure 9b). The dimensionless rate constant of 0.13 is equivalent to $k^0 = 3.7 \times 10^{-3}$ cm/s with $a = 5.0$ μm and $D = 3.6 \times 10^{-6}$ cm^2/s for $Co(phen)_3^{2+}$ as determined by chronoamperometry[43] (see eq 10). The kinetic parameters agree with $k^0 = 4.0 \times 10^{-3}$ cm/s and $\alpha = 0.4$ as obtained from a quasi-reversible voltammogram at the carbon fiber substrate (data not shown). This good agreement confirms that a standard rate constant of electron transfer at an unbiased substrate can be determined by SECM when the SECM geometries are such that the substrate potential remains around the formal potential during the tip approach. The standard rate constant is intermediate between 8×10^{-2} cm/s at a laser-activated glassy carbon electrode and 2×10^{-5} cm/s at a highly ordered pyrolytic graphite electrode.[44]

With $Co(phen)_3^{2+}$ as a quasi-reversible mediator, the overpotential at the small substrate is nearly constant during the approach curve measurement ($E - E^0 \sim -0.025$ V in Figure 9b). Therefore, the electron transfer rate at the unbiased substrate is practically independent of the tip–substrate distance. This situation is similar to that of a biased substrate at a constant potential. Well-developed theory for biased substrates,[25,35] however, is not applicable to an unbiased substrate, where the feedback current depends on the substrate size and tip outer radius. Furthermore, the negative approach curve for the slow substrate reaction resembles that of a reversible reaction with a small substrate radius and/or a thick insulating sheath of a tip. For a quasi-reversible process at an unbiased substrate, numerical simulations with knowledge of the b/a and RG values are required for determination of kinetic parameters from a current approach curve.

SECM Imaging

The numerical simulations of line scan above an unbiased disk substrate predict that the tip current is smaller above the center of the substrate than above the edges (Figure 6a). Such a current dip was observed in a SECM image of the disk carbon fiber electrode at open circuit potential (Figure 10a), where a 10 μm-diameter disk Pt electrode with RG = 8 was scanned at

30 μm/s. The tip current in the image was recorded only when the probe was moved from the left-hand side of the substrate to the right-hand side. Despite the symmetric substrate and tip geometries, the current response in the image is not symmetric with respect to the substrate center. As the probe was scanned across the substrate from the left-hand side to the right-hand side, the tip current was enhanced more above the left edge than above the right edge. Similar asymmetric images were reported previously, where a pair of disk UMEs with the same diameter were used as a tip and an unbiased substrate.[22] In the previous report, the asymmetric line scans with a current dip above the substrate center were ascribed to a transient response because the asymmetry was enhanced as the probe scan rate increased from 5 μm/s to 200 μm/s.

As predicted theoretically, however, the current dip above the substrate center was still observed, even at a very slow scan rate of 0.05 μm/s (solid lines in Figure 10b). In contrast to the line scan at the rate of 5 μm/s (dotted lines in Figure 10b), the symmetric line scan at the slow scan rate confirms the steady state. The larger current response above the substrate edge is due to higher accessibility of the substrate edge to the mediator in the bulk solution when the tip is positioned above the other side of the substrate edge (Figure 6b). A current dip above the substrate center is smaller with the 10 μm-diameter probe with RG = 2 (Figure 10b). When a probe with smaller RG is positioned above the substrate center, mediator diffusion from the bulk solution to the substrate edge is less hindered by the insulating sheath of the tip.

The current dip is not due to slower mediator generation at the substrate center than at the edge. As the tip is brought to the substrate center at slow scan rates, the approach curves with 1,1′-ferrocenedimethanol fit with theoretical curves for a reversible substrate reaction (Figures 7–9). Importantly, not only the tip but also the substrate must be small enough to achieve a steady state without convection effect at an unbiased substrate. Mediator electrolysis at an unbiased substrate results in a concentration gradient of the mediator from the substrate edge to the bulk solution, where the thickness of the diffusion layer is determined by the substrate size rather than by the tip size.

CONCLUSIONS

SECM feedback at an unbiased substrate was quantified theoretically for the case of a pair of disk UMEs as the tip and the substrate. At the unbiased substrate, both tip current and substrate potential depend on SECM geometries with respect to the tip radius including the tip–substrate distance, substrate radius, and thickness of the insulating sheath of the tip. A larger feedback effect is obtained using a probe with a thinner insulating sheath, enabling detection of a smaller active spot. The feedback current at an unbiased substrate, however, is much smaller than that at a biased substrate with the same size. Therefore, a probe with a smaller outer diameter[40,45] will be useful for SECM studies of unbiased conductors.

A slower rate of heterogeneous electron transfer at an unbiased substrate results in a smaller feedback current. This trend is qualitatively similar to that of biased substrates. The SECM theory for biased substrates,[25,35] however, is not applicable for unbiased substrates, where the feedback effect strongly depends on the SECM geometries. Numerical simulations of an approach curve with the geometrical parameters allow the determination of a standard rate constant of electron transfer at an unbiased substrate when the transfer coefficient is known or when the substrate is small enough that the substrate potential remains close to the formal potential during the tip approach.

The theoretical approach reported here will be useful also for other SECM systems. The substrate radius and tip outer radius would also affect the tip current that is controlled by lateral electron transport through an unbiased substrate with finite conductivity.[10,20] The theory will

be extendable also to SECM feedback based on ion transfer at an externally unbiased interface between two liquid phases.[16,29,33]

Supplementary Material

Refer to Web version on PubMed Central for supplementary material.

Acknowledgements

We thank the National Science Foundation (DBI0242561) and the National Institute of Health (GM073439) for their financial support. This work was also supported by the University of Pittsburgh. We appreciate the assistance of Darrick A. Gross for his preliminary studies. The authors thank Gregg P. Kotchey for his comments on the manuscript.

References

1. Bard, AJ.; Mirkin, MV., editors. Scanning Electrochemical Microscopy. Marcel Dekker; New York: 2001.
2. Barker AL, Gonsalves M, Macpherson JV, Slevin CJ, Unwin PR. Anal Chim Acta 1999;385:223–240.
3. Amemiya S, Guo J, Xiong H, Gross DA. Anal Bioanal Chem 2006;386:458–471. [PubMed: 16855816]
4. Bard AJ, Fan FRF, Kwak J, Lev O. Anal Chem 1989;61:132–138.
5. Bard AJ, Zoski CG. Anal Chem 2000;72:346A–352A.
6. Quinn BM, Prieto I, Haram SK, Bard AJ. J Phys Chem B 2001:7474–7476.
7. Wang J, Song F, Zhou F. Langmuir 2002;18:6653–6658.
8. Liljeroth P, Quinn BM, Ruiz V, Kontturi K. Chem Commun 2003:1570–1571.
9. Ruiz V, Liljeroth P, Quinn BM, Kontturi K. Nano Letters 2003;3:1459–1462.
10. Liljeroth P, Vanmaekelbergh D, Ruiz V, Kontturi K, Jiang H, Kauppinen E, Quinn BMJ. Am Chem Soc 2004;126:7126–7132.
11. Fernandez JL, Hurth C, Bard AJJ. Phy Chem B 2005;109:9532–9539.
12. Ruiz V, Nicholson PG, Jollands S, Thomas PA, Macpherson JV, Unwin PRJ. Phys Chem B 2005;109:19335–19344.
13. Liljeroth P, Quinn BM. J Am Chem Soc 2006;128:4922–4923. [PubMed: 16608304]
14. Wilson NR, Guille M, Dumitrescu I, Fernandez VR, Rudd NC, Williams CG, Unwin PR, Macpherson JV. Anal Chem 2006:7006–7015. [PubMed: 17007527]
15. Xiong H, Gross DA, Guo J, Amemiya S. Anal Chem 2006;78:1946–1957. [PubMed: 16536432]
16. Guo J, Amemiya S. Anal Chem 2005;77:2147–2156. [PubMed: 15801749]
17. Mandler D, Unwin PR. J Phys Chem B 2003;107:407–410.
18. Zhang J, Barker AL, Mandler D, Unwin PR. J Am Chem Soc 2003;125:9312–9313. [PubMed: 12889958]
19. O'Mullane AP, Macpherson JV, Unwin PR, Cervera-Montesinos J, Manzanares JA, Frehill F, Vos JG. J Phys Chem B 2004;108:7219–7227.
20. Whitworth AL, Mandler D, Unwin PR. Phys Chem Chem Phys 2005;7:356–365.
21. Wipf DO, Bard AJ. J Electrochem Soc 1991;138:469–474.
22. Macpherson J, Slevin CJ, Unwin PR. J Chem Soc, Faraday Trans 1996;92:3799–3805.
23. Selzer Y, Turyan I, Mandler DJ. Phys Chem B 1999;103:1509–1517.
24. Zoski CG, Simjee N, Guenat O, Koudelka-Hep M. Anal Chem 2004;76:62–72.
25. Wei C, Bard AJ, Mirkin MVJ. Phys Chem 1995;99:16033–16042.
26. O'Mullane AP, Neufeld AK, Bond AM. Anal Chem 2005;77:5447–5452. [PubMed: 16131051]
27. Ghilane J, Hauquier R, Fabre B, Hapiot P. Anal Chem 2006;78:6019–6025. [PubMed: 16944879]
28. Peterson RR, Cliffel DE. Langmuir 2006;22:10307–10314. [PubMed: 17128997]
29. Shao Y, Mirkin MVJ. Phys Chem B 1998;102:9915–9921.
30. Zoski CG, Mirkin MV. Anal Chem 2002;74:1986–1992. [PubMed: 12033296]

31. Bard, AJ.; Faulkner, LR. Electrochemical Methods: Fundamentals and Applications. 2. John Wiley & Sons; New York: 2001. p. 94-96.
32. Bard AJ, Mirkin MV, Unwin PR, Wipf DO. J Phys Chem 1992;96:1861–1868.
33. Selzer Y, Mandler DJ. Phys Chem B 2000;104:4903–4910.
34. Kwak J, Bard AJ. Anal Chem 1989;61:1221–1227.
35. Bard AJ, Mirkin MV, Unwin PR, Wipf DOJ. Phys Chem 1992;96:1861–1868.
36. Chen YWD, Santhanam KSV, Bard AJ. J Electrochem Soc 1982;129:61–66.
37. Wightman, RM.; Wipf, DO. Electroanalytical Chemistry. Bard, AJ., editor. 15. Marcel Dekker; New York: 1989. p. 267-351.
38. Fan, F-RF. Scanning Electrochemical Microscopy. Bard, AJ.; Mirkin, MV., editors. Marcel Dekker; New York: 2001. p. 111-143.
39. Amemiya S, Bard AJ. Anal Chem 2000;72:4940–4948. [PubMed: 11055713]
40. Xiong H, Guo JD, Kurihara K, Amemiya S. Electrochem Commun 2004;6:615–620.
41. Bourdillon C, Demaille C, Moiroux J, Saveant JMJ. Am Chem Soc 1995;117:11499–11506.
42. Amphlett JL, Denuault GJ. Phys Chem B 1998;102:9946–9951.
43. Denuault G, Mirkin MV, Bard AJJ. Electroanal Chem 1991;308:27–38.
44. Cline KK, McDermott MT, McCreery RLJ. Phys Chem 1994;98:5314–5319.
45. Liu B, Rolland JP, DeSimone JM, Bard AJ. Anal Chem 2005;77:3013–3017. [PubMed: 15859625]

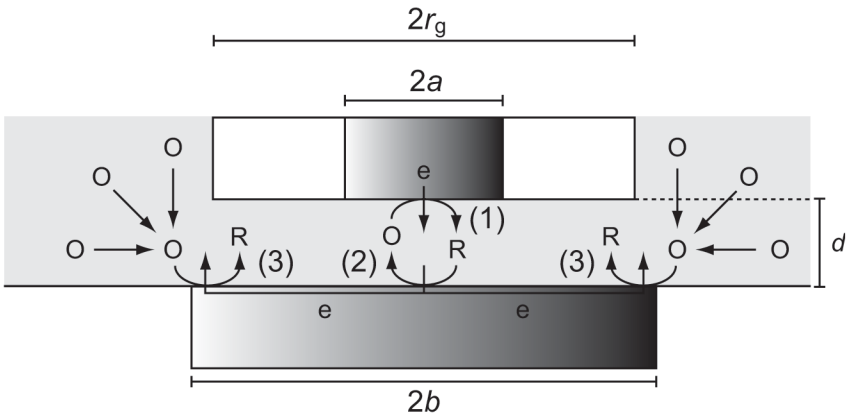

Figure 1.
Scheme of a SECM feedback experiment with a disk UME probe positioned above a disk substrate electrode at open circuit potential.

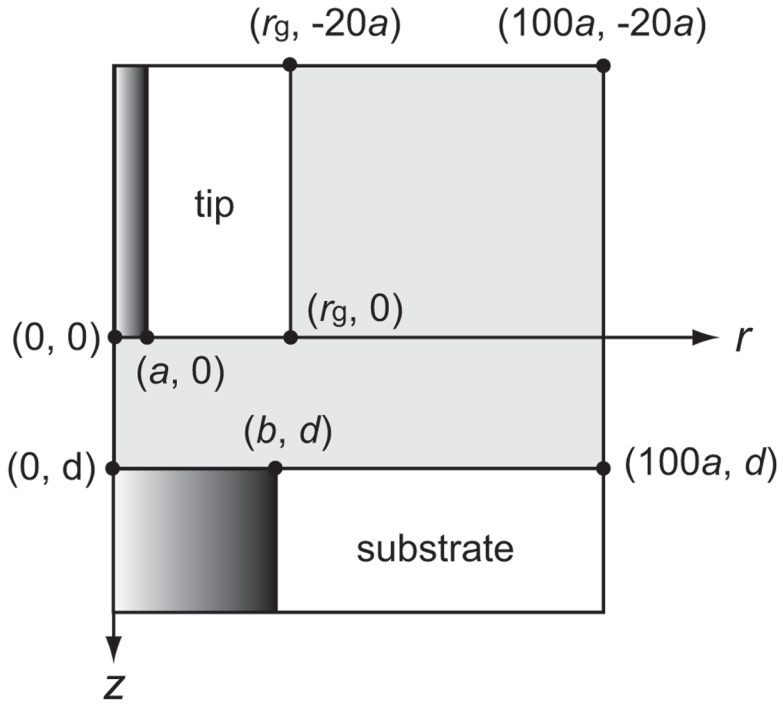

Figure 2.
Geometry of the SECM diffusion problem in a cylindrical coordinate.

(a)

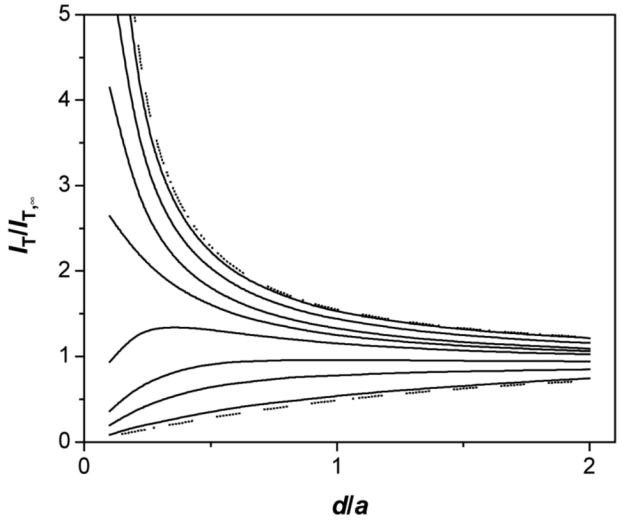

(b)

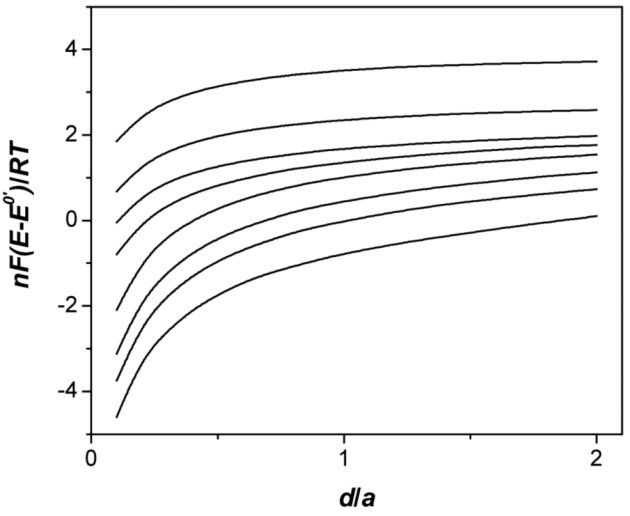

(c)

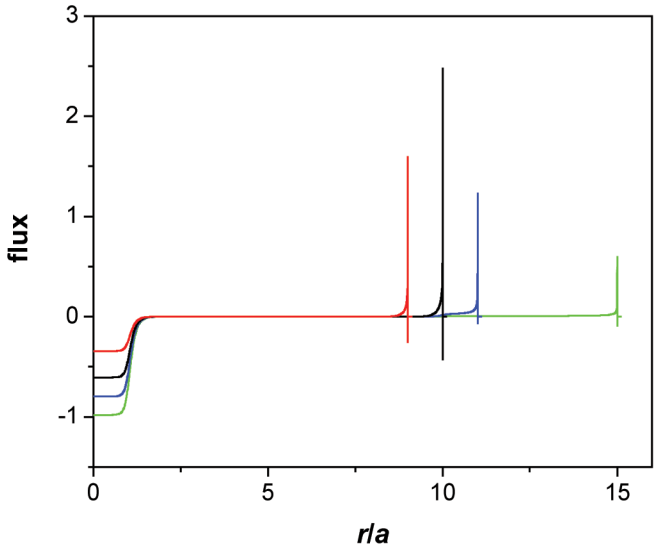

Figure 3.

Effect of the substrate radius on (a) current and (b) potential approach curves with a disk UME probe with RG = 10. The solid lines are for *b/a* = 30, 15, 11, 10, 9, 7, 5, and 2 from the top. The upper and lower dotted lines in (a) represent theoretical approach curves with conductive and insulating substrates, respectively.[29] (c) Distribution of interfacial mediator flux at the surface of unbiased substrates with *b/a* = *9* (red), 10 (black), 11 (blue), and 15 (green) under a disk probe with RG = 10. The flux at the substrate surface is given in the dimensionless form as 0.25 $[\partial C(\mathrm{R,Z})/\partial Z]_{\mathrm{Z=L}}$ (see Supporting Information for definitions of dimensionless parameters).

(a)

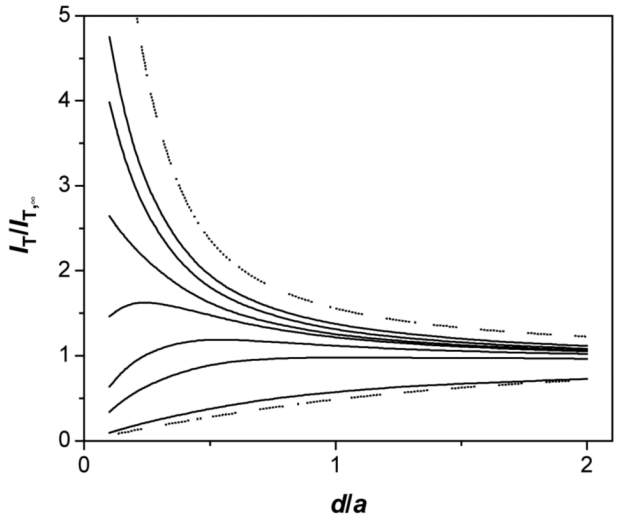

(b)

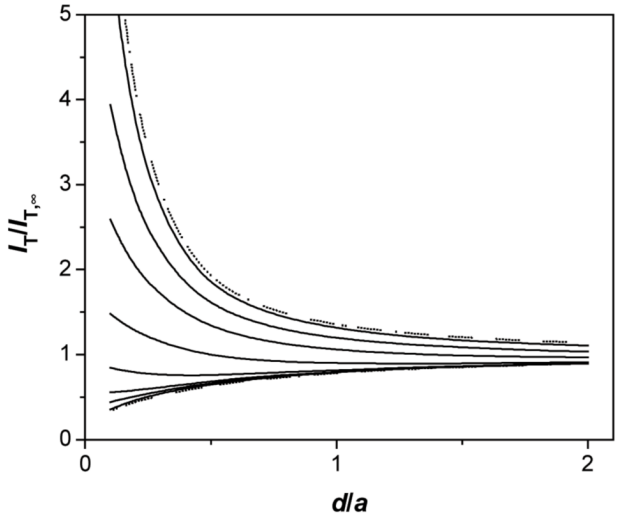

Figure 4.

A RG effect on current approach curves with unbiased disk substrates as simulated for disk UME probes: (a) *b/a* = 10 and RG = 1.1, 6, 9, 10, 10.5, 12, 15, 50 from the top, and (b) RG = 1.1 and *b/a* = 30, 10, 5, 2.5, 1.5, 1.2, 1.1, and 1.0 from the top. The upper and lower dotted lines represent theoretical approach curves with conductive and insulating substrates, respectively.[29] The corresponding potential approach curves are shown in Supporting Information.

(a)

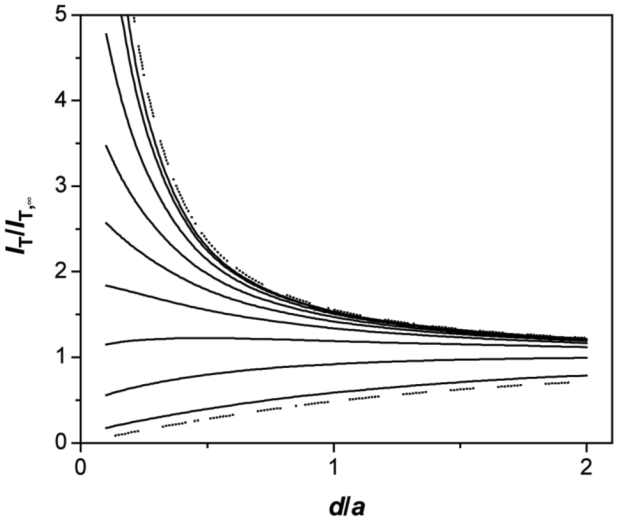

(b)

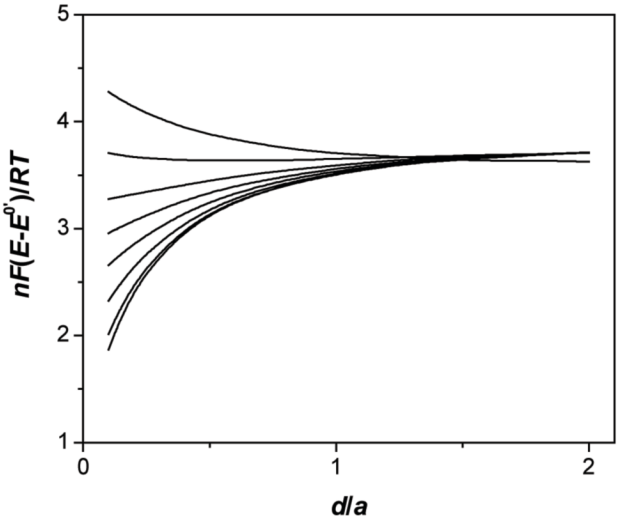

Figure 5.

Effect of the intrinsic rate of the substrate reaction on (a) current and (b) potential approach curves with an unbiased disk substrate with b/a = 30 under a disk UME probe with RG = 10. The solid lines are for K = 10, 1, 0.25, 0.1, 0.05, 0.025, 0.01, 0.0025, and 0.00025 from (a) the top and (b) the bottom. The upper and lower dotted lines in (a) represent theoretical approach curves with conductive and insulating substrates, respectively.[29]

(a)

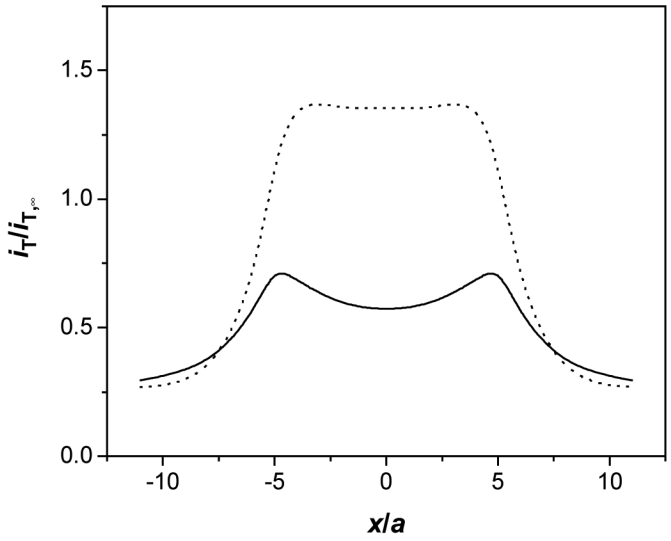

(b)

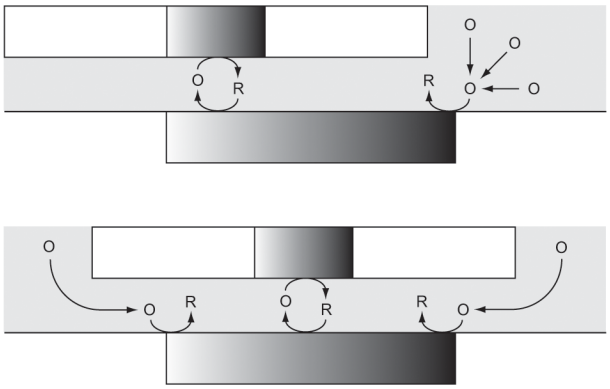

Figure 6.

(a) Tip currents in line scans over an unbiased disk substrate with b/a = 5 as simulated for a disk probe with RG = 10 (solid line) and 4 (dotted line) at d/a = 0.5. (b) Scheme of mediator diffusion from the bulk solution to the substrate edge when the tip is positioned above the edge (top) and the center (bottom) of the substrate.

(a)

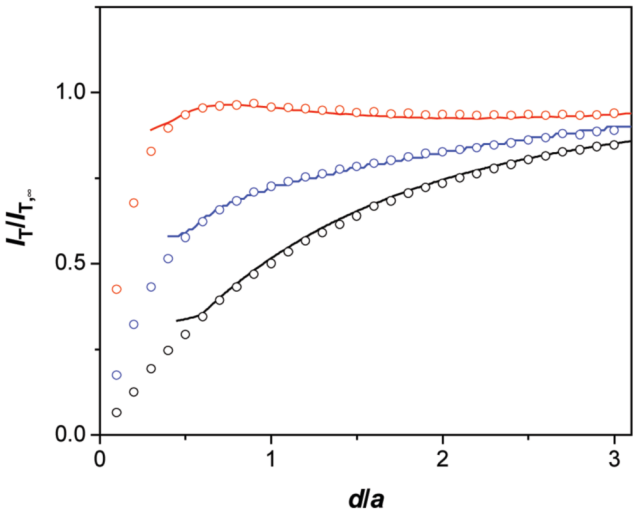

(b)

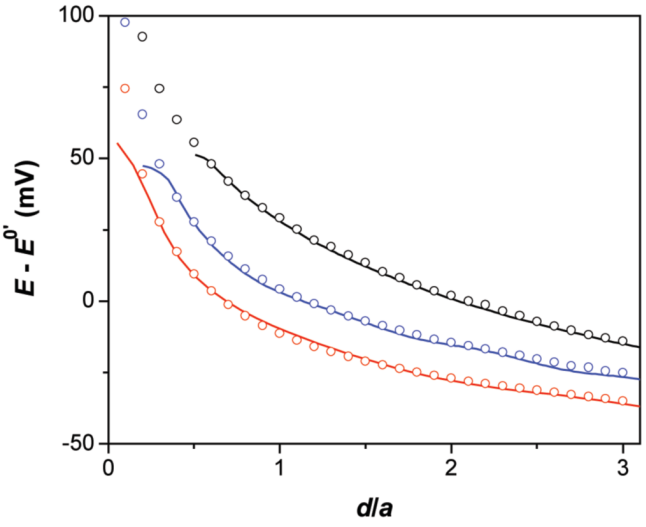

Figure 7.

(a) Current and (b) potential approach curves at an unbiased disk carbon fiber substrate as obtained using disk Pt probes with 1 mM 1,1′-ferrocenedimethanol in 0.1 M KCl. The circles and solid lines represent the experimental and theoretical curves, respectively, (*a*, *b/a*, RG) = (12.5 μm, 1.29, 10.0), (5.0 μm, 3.65, 8.0), and (3.0 μm, 5.61, 7.5) were used for the data in red, blue, and black. The tip potential: 0.4 V versus Ag/AgCl. The probe scan rate: 1.5 μm/s for *a* = 12.5 μm, and 0.6 μm/s for *a* = 5.0 and 3.0 μm.

(a)

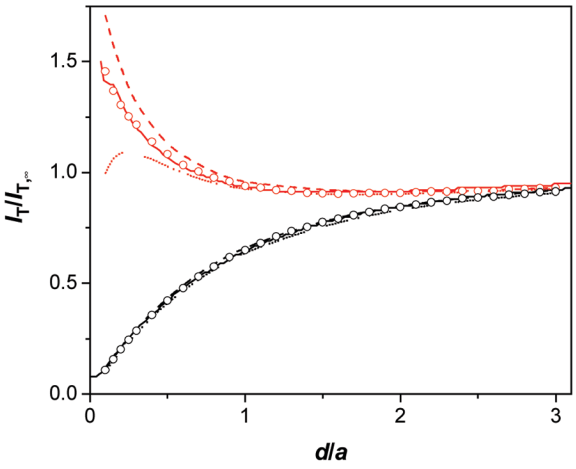

(b)

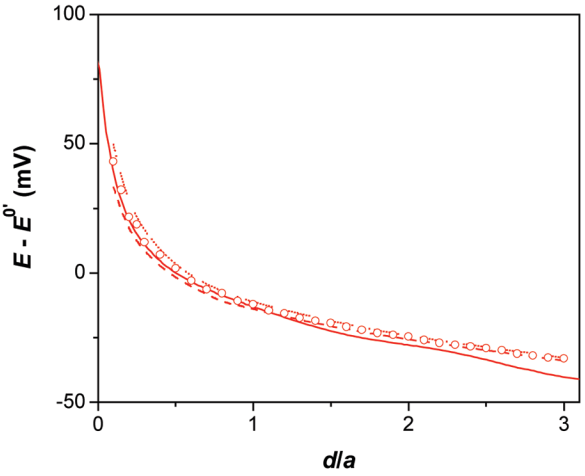

Figure 8.

(a) Current approach curves at a 34 μm-diameter disk carbon fiber electrode at open circuit potential (red) and at a Teflon substrate (black) as obtained using a 10 μm-diameter Pt disk probe with RG = 3.3. (b) The corresponding potential approach curve at the carbon fiber substrate. The solid lines represent the experimental curves. The circles, dashed line, and dotted line represent theoretical curves with RG = 3.3, 3.1, and 3.5, respectively. The approach curves were measured with 1 mM 1,1′-ferrocenedimethanol in 0.1 M KCl. The tip potential: 0.4 V versus Ag/AgCl. The probe scan rate: 0.6 μm/s.

(a)

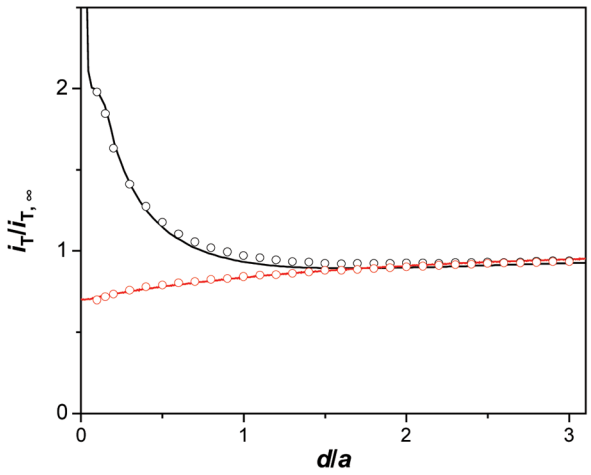

(b)

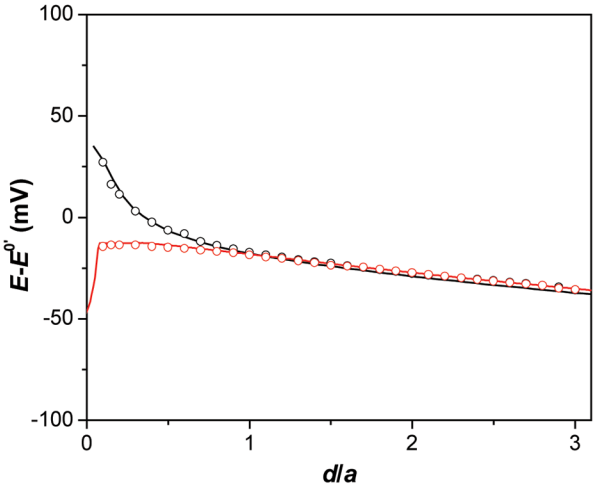

Figure 9.

(a) Current and (b) potential approach curves with 1 mM 1,1′-ferrocenedimethanol (black) and 2 mM $Co(phen)_3^{2+}$ (red) in 0.1 M KCl with the 34 μm-diameter disk carbon fiber substrate at open circuit potential as obtained using a 10 μm-diameter Pt disk probe with RG = 2.0. The circles and solid lines represent the experimental and theoretical approach curves, respectively. The theory curve for 1,1′-ferrocenedimethanol is based on a reversible substrate reaction. The theory curve for $Co(phen)_3^{2+}$ was obtained for $K = 0.52$ with $\alpha = 0.5$. The tip potential: 0.4 and 0.3 V versus Ag/AgCl for 1,1′-ferrocenedimethanol and $Co(phen)_3^{2+}$, respectively. The probe scan rate: 0.6 μrn/s.

(a)

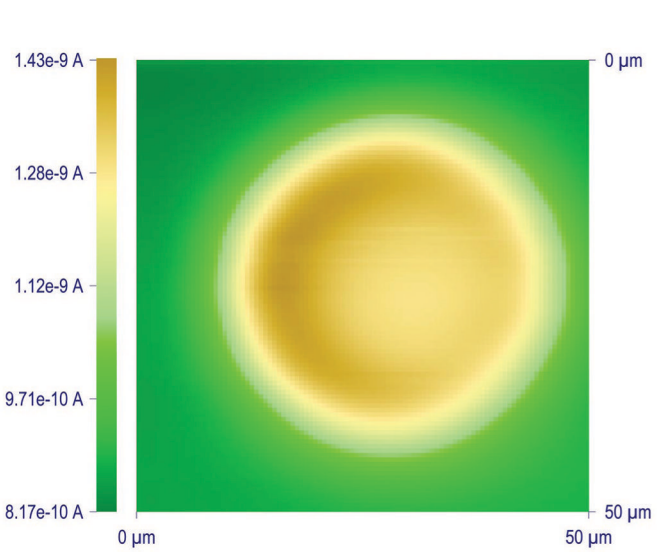

(b)

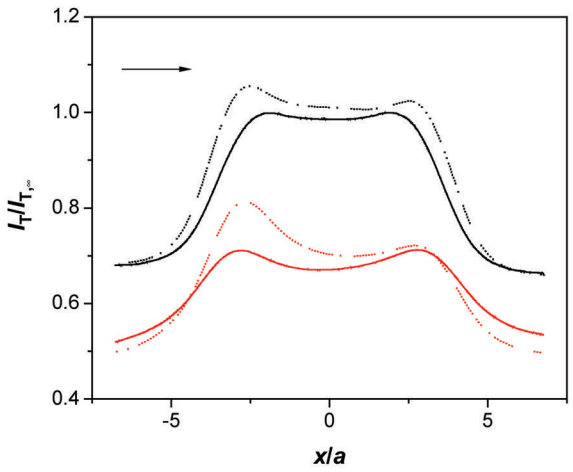

Figure 10.

(a) SECM images of a ~33 µm-diameter carbon fiber disk electrode at open circuit potential as obtained using a 10 µm-diameter Pt disk probe with RG = 8 with 1 mM 1,1′-ferrocenedimethanol in 0.1 M KCl. The probe scan rate: 30 µm/s. (b) SECM line scans over the unbiased substrate at the scan rate of 0.05 (solid line) and 5 (dotted line) µm/s as obtained using 10 µm-diameter Pt disk probes with RG = 8 (red) and 2 (black). The arrow indicates the scan direction. The tip potential: 0.4 V versus Ag/AgCl. The lateral tip position, *x*, is arbitrary.